An SRTM assisted image matching algorithm for long-strip satellite imagery

XIONG Jinxin, ZHANG Yongjun, ZHENG Maoteng, YE Yuanxin

School of Remote Sensing and Information Engineering, Wuhan University, Wuhan 430079, *China*

Abstract: Faced with the problem of unstable reliability in matching long-strip imagery of Chinese satellite, a matching algorithm is presented using the global Shuttle Radar Topography Mission (SRTM) data as elevation control. First, this algorithm employs the block partition mechanism, and introduces Local Binary Pattern/Contrast (LBP/C) operator to filter the interest points. Second, the global SRTM data is used to compute the true topographic relief within the image coverage. Based on the true topographic relief, the approximate epipolar line is constructed and the accuracy is analyzed. Third, on the pyramid level, two-dimensional correlation matching is executed to search for the optimal matches along the epipolar line. During the matching process, the geometry rectification method is applied to improve the accuracy of matching. Finally, on the original level, Multi-Photo Geometrically Constrained (MPGC) matching algorithm is adopted to refine the matching result, and Random Sample Consensus (RANSAC) is imbedded to eliminate mismatches. In order to ensure the distribution uniformity of matches, the region-growing algorithm is introduced. The main advantage of the proposed algorithm is that it can realize the automatic matching for long-strip imagery of different Ground Sample Distance (GSD), different visual angles in parallel environment. Through the comparison between the proposed method and the mainly existing methods, the results show that the matching accuracy is improved.

Key words: long-strip, SRTM, image matching, Mapping Satellite-1, ZY-3

CLC number: P23 **Document code:** A

Citation format: Xiong J X, Zhang Y J, Zheng M T and Ye Y X. 2013. An SRTM assisted image matching algorithm for long-strip satellite imagery. Journal of Remote Sensing, 17(5): 1103-1117 [DOI: 10.11834/jrs.20132224]

1 INTRODUCTION

With the rapid development of space technology and the important breakthrough of satellite positioning technique, the number of satellites in orbit has risen dramatically. Nowadays More and more satellite data are applied in photogrammetric and remote sensing field (Cheng, et al., 2010). The imaging principle of CCD push-broom satellite can well avert the image matching abnormality (Zhu, et al., 2005). Due to the position and attitude parameters provided by the satellite data (Zhang, et al., 2013), the approximate epipolar line can be constructed as a geometric constraint, which improves the accuracy and stability of image matching. Most of the satellite sensors generally work in push broom mode and capture continuous strips of images, in which the incomplete central projection exists. This imaging mode is more complicated than that with central projection. At present, multi-CCD linear array model is applied on the satellites in order to provide multi-view data, so images with different intersection angles, focal lengths and GSD can be obtained. However, a n umber of problems have arisen in the meantime, such as n onlinear geometric and radiometric distortions, which leads to decrease in efficiency and reliability of the existing matching methods. These problems have brought enormous challenge.

Zhu (2011) improved the Scale-Invariant Feature Transform (SIFT) algorithm, which could solve problems of the large m emory consumption and slow operation. This improved method can work in parallel environment and increase the accuracy of matching to a certain extent. However, this method may not be suitable to process large satellite data. Li (2010) proposed a f eature matching method which was constrained by line features and achieved high accurate matching location of point features. This method needs accurate line features, but it is hard to extract these lines on satellite images. Ji (2010) proposed a multi-resolution matching strategy, which could automatically match with multiple satellite images through predicting initial matches based on Rational Function Model (RFM). But its correct rate of matching may not be high enough, and the accuracy needs to be i mproved. Zhang (2006) presented a automatical matching procedure for Digital Surface Model (DSM) generation from linear a rray satellite imagery, which provided dense, precise, and reliable results. He used a coarse-to-fine hierarchical strategy, and effectively combined with several image matching

Received: 2012-07-27; **Accepted:** 2013-04-11; **Version of record first published:** 2013-04-18

Foundation: National High Technology Research and Development Program of China (863 Program) (No. 2012AA12A301, 2013AA12A401); National Natural Science Foundation of China (No. 41071233); The Fundamental Research Funds for the Central Universities (No. 201121302020004); Academic Award for Excellent Ph. D. Candidates Funded by Ministry of Education of China (No. 5052011213018)

First author biography: XIONG Jinxin (1987—), male, Ph. D. candidate. He majors in space and aerial photogrammetry, combined multi-view matching algorithm with multi-source imagery. E-mail: einbetter1995@ hotmail. com

Corresponding author biography: ZHANG Yongjun (1975—), male, professor. His research interests are digital photogrammetry, remote sensing, and computer vision. E-mail: zhangyj@ whu. edu. cn

algorithms. Additionally, a modified MPGC matching algorithm was adopted to obtain sub-pixel accuracy. Silveira (2008) proposed a concept which integrated gray scale-based matching with feature-based matching. This approach utilized SIFT operator to obtain a series of initial matches, and then adopted Least Squares Matching (LSM) based on a regional-growing algorithm to generate the final matches.

Analysis indicates that the existing matching algorithms mainly process the foreign satellite with highly accurate Global Positioning System (GPS) position and attitude parameters, and most of the work focus on scenes along the same track or adjoining track. However, for the Chinese satellites, there are some characteristics different from the foreign satellites. First, the attitude positioning technique is not fully developed yet, so that the accuracy of direct positioning is limited (Xie, 2009). Second, images captured by Chinese satellites have poor information quantity, and textural features are not abundant enough. Finally, the direct transfer data is continuous long-strip images, once the images are processed as scenes, after bundle block adjustment, the accuracy of direct positioning is hard to keep consistent between scenes, which lead to the mosaic gaps in image merging. Consequently, processing long-strip images rather than scenes, will be a better option.

This paper develops a practical matching algorithm based on the global SRTM data. First, a long-strip image that most close to vertical photography is taken as a reference image, and divided into blocks. These blocks are overlapping and independent on each other. First, we use Harris operator (Harris & Stephens, 1998) to extract feature points on reference blocks. Second, LBP/C measure (Timo & Matti, 2002) is introduced to select the optimal features, which needs to include strong texture information and high contrast. Then, through the global SRTM data, the true topographic relief is obtained. Finally, the approximate epipolar is constructed based on the actual topographic relief. Along the epipolar, local geometric and radiometric distortion is corrected. This algorithm employs image pyramid strategy to reduce computing burden, from the top level to the original level, forward intersection with multi-image method is used to compute the object coordinates of corresponding feature points, and then Digital Surface Model (DSM) is constructed for refining SRTM elevation and refreshing local distortion parameters. As initial information, this result is transferred to the lower level, which can reduce search window size and improve prediction precision of the epipolar line. Till to the original level, the matching result is taken as experience value, and region-growing method (Xiong, 2009) is introduced to encrypt feature points and ensure the uniform distribution in region of poor texture. MPGC algorithm (Gruen, et al., 1988) is adopted to refine the coordinates of matches, and bundle forward intersection (Zhang & Hu, 2007) is used to detect and eliminate the mismatches. Fig. 1 shows the general strategy of the proposed algorithm.

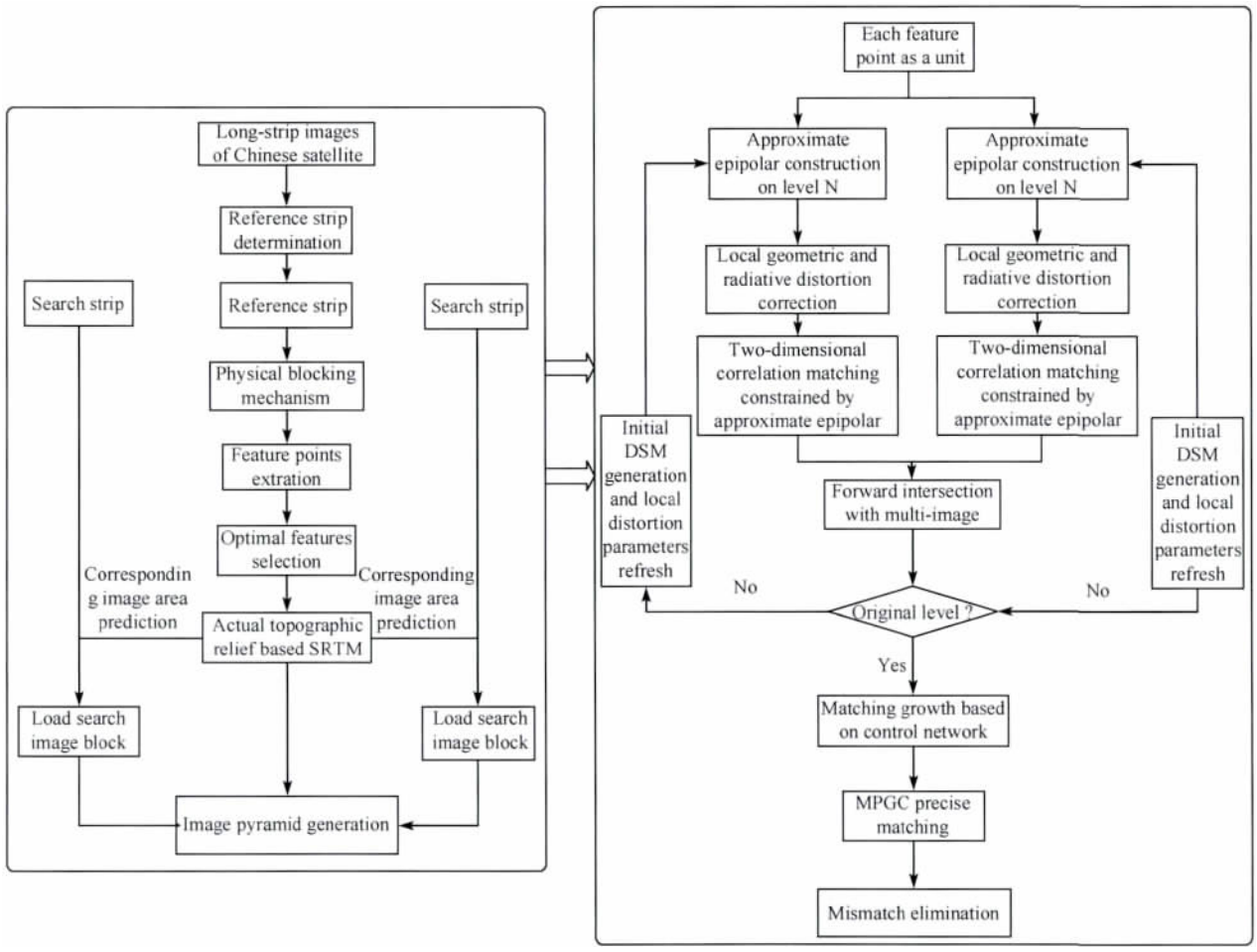

Fig. 1 The general strategy of combined matching algorithm assisted global SRTM

2 METHODOLOGY

2.1 Physical blocking mechanism

Due to the large datasets of long-strip images, these data can not be loaded into internal storage one time. Therefore, we separate them into independently overlapping blocks. This strategy provides the possibility of constructing a scheme of parallel matching, and the subsequent procedures are all based on blocks.

In this study, we set the size of a block to 12000 × 12000 pixels. If the blocks are close to an image edge and images are divided across a border, the size will be shrunken or broadened with adaptive control. In this procedure, we construct an index record of all the image patches to find their corresponding original strips.

Fig. 2 shows the results of the physical blocking mechanism. In consideration of the continuous boundaries between blocks, there was about a 10% overlap.

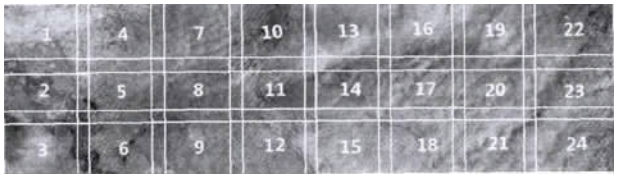

Fig. 2 Example of blocking partition

Fig. 2 shows a long-strip divided into 24 image blocks; each rectangle represents the size of the corresponding block, which was determined by adaptive control. There was a certain degree of overlap between adjacent blocks.

2.2 Optimal features selection

Cheng, et al. (2008) indicated that the strong relationship exists between matching accuracy and the texture information content. Although detailed rules differ by surface variations, it has been shown that matching accuracy will increase when an image have abundant texture information and high contrast.

As a powerful tool for texture classification, the Local Binary Pattern (LBP) operator is an excellent measure of the s patial structure of local image texture. LBP operator allows for detecting "uniform" patterns in circular neighborhood. This c ircular neighborhood can be invariant under the difference of angular space and spatial resolutions. Moreover, through combining with a rotation invariant Local Contrast (LC) measure, the performance of the LBP operator is enhanced. LBP/C operator can well analyze spatial characteristic and contrast for local texture information. Therefore, using LBP/C operator to select optimal features may effectively improve the correct rate of matching.

In this paper, feature points are extracted by Harris operator. After extracting the feature points, we utilize LBP/C operator to compute LBP value and LC value of all features. Then Two-d imensional histogram is defined as distributed statistics of the two values. This describes local space characteristic and contrast of every feature point. To testify the performance of the method above mentioned, two sets of stereo images respectively acquired from Mapping Satellite-1 and ZY-3 are used as test data, and a total of 287 check points are picked up. As feature points, these check points are used to judge the correct rate of matching.

Fig. 3 shows the histogram statistics in areas with abundant and poor texture information respectively. When check points l ocate in area with poor texture information, LC value is close to zero. Table 1 describes the matching results, and the correct rate of matching in area with abundant texture information is obviously higher. So this method is effective to eliminate unstable feature points.

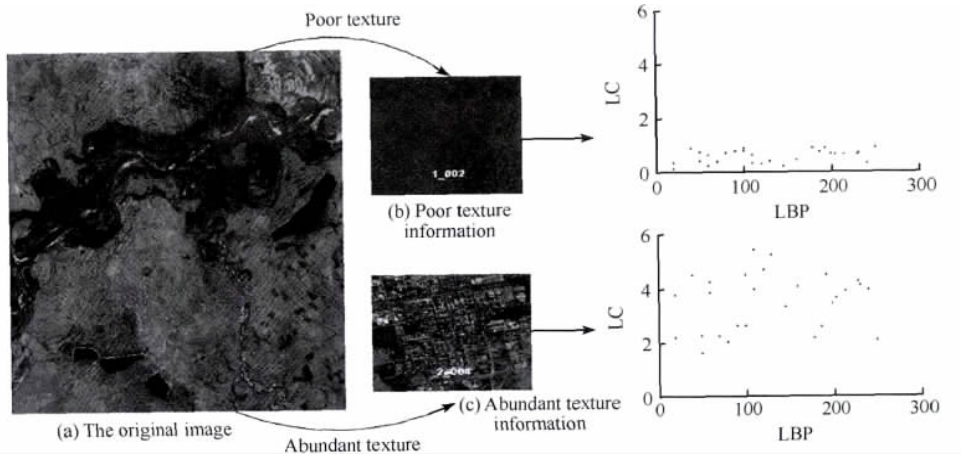

Fig. 3 The histogram of LBP/C

Table 1 Comparison of matching performance for different texture information

Satellite	Texture area	Number of check points	Successful rate/%	Correct rate/%
Mapping Satellite-1	Poor texture	47	70.2	51.5
	Abundate texture	86	79.0	75.3
ZY-3	Poor texture	61	75.4	61.2
	Abundate texture	93	93.5	82.9

2.3 Actual topographic relief based on SRTM data

The satellite imaging system works in push broom mode. It projects an image onto a linear array of sensors, typically a CCD line array. Every scan line has its own projection centre and attitude parameters, so there is no rigorous epipolar (Ji & Yuan, 2010). Zhang (2011) discussed the relationship between elevation error and matching accuracy, and indicated that the less of

difference between initial elevation and actual value, the better in matching accuracy. To remove the influence on prediction of a pproximate epipolar line, initial elevation is achieved through global SRTM data. Using the elevation relief, the approximate epipolar line is generated as the constraint condition.

According to the position and attitude information of the scan lines, we used a hypothetical height to the frontal-project four corners of the corresponding reference image patch onto the ground. The approximate geography scope covered by the image patch was determined, and the maximum elevation H_{max} and the minimum elevation H_{min} are achieved through retrieval from Global DEM.

We frontal-projected an interest point extracted onto the ground using H_{max} and H_{min}, and back-projected these object space points onto all of the search long-strip images. The corresponding image coordinates (x_{max}, y_{max}), (x_{min}, y_{min}) then could be determined. After that, we calculated the elevation step H_{pitch} and elevation value H_i with the following equation:

$$H_{pitch} = (H_{max} - H_{min}) / Length \quad (1)$$

$$Length = \sqrt{(x_{max} - x_{min})^2 + (y_{max} - y_{min})^2} \quad (2)$$

$$H_i = H_{min} + i \cdot H_{pitch} (i = 1, 2, \cdots, n, H_i \leqslant H_{max}) \quad (3)$$

2.4 Approximate epipolar-constrained matching strategy

As a feature point, once its approximate epipolar line on the search long-strip image is generated, the corresponding point should locate on the epipolar line theoretically. The matching strategy only needs to use One-dimensional correction matching algorithm along the epipolar. However, the approximate epipolar line includes prediction error. There is some deviation between the position of the actually corresponding point and the epipolar line. Prediction error includes lens distortion of camera, error of direct location and elevation error of SRTM data. To quantify the prediction error, forward-view and backward-view images r espectively acquired from Mapping Satellite-1 and ZY-3 are used as two test stereo images. A total of 36 check points are picked up. Table 2 describes the error statistic, and in this table, the deviation is equal to the distance of the actual point position and the nearest neighbor of the epipolar line.

Table 2 The list of prediction error statistic

Stereo images	Number of check points	Maximum deviation in X direction /(pixel)	Mean deviation in X direction /(pixel)	Maximum deviation in Y direction /(pixel)	Mean deviation in Y direction /(pixel)
First stereo	15	10.2	4.8	85.5	76.3
Second stereo	21	54.6	32.2	44.9	25.1

Table 2 indicates that the maximum deviation in X direction is about 54 pixels, and in Y direction, the max deviation is more than 85 pixels. It is effective to introduce pyramid matching strategy. The accuracy of matching is refined through reducing search scope on successive levels. In this paper, the matching strategy takes 3 ×3 pixels as a template, three pyramid levels are generated by median filter. The relative window on top level is 5 ×5 pixels, and the search window size is 11 pixels in X direction, and 35 pixels in Y direction. Normalized correlation coefficient is used as similarity measure, the threshold is 0.65. Along the approximate epipolar line, all candidate points, whose correlation coefficient is more than 0.65, are fitted by conic fitting method. The maximum in the curve is determined as the initial match. Passed through level by level, the search window in each level is 2 ×6 pixels smaller, and the threshold is 0.05 higher. The search window size is 5 ×13, the threshold is set to 0.8 on the o riginal level.

There are geometric and radiometric distortions in the case of strips acquired from different camera lenses. When the correlation window is defined in the reference image, distortion leads to an irregular and discontinuous shape of the corresponding window in the search images, which cannot be matched directly.

In the reference block, we define a correlated window Π and a search window Γ in which an feature point or candidate was central, then the corresponding pixel coordinates of the four corners and the center of Γ are achieved by projection in the search image, which form an irregular polygon $\sum_P$, as shown in Fig. 4. Accordingly, we calculate the parameters of the affine g eometric transformation and linear radiometric transformation between these images.

$$x_2 = a_0 + a_1 x + a_2 y \quad (4)$$

$$y_2 = b_0 + b_1 x + b_2 y \quad (5)$$

$$g(x, y) = h_0 + h_1 g_2(x_2, y_2) \quad (6)$$

where a_0, a_1, a_2, b_0, b_1, b_2 are the parameters of the affine g eometric transformation; h_0, h_1 are the parameters of the linear radiometric transformation.

Through Eq. 3 and Eq. 4, the relationship of each pixel b etween Γ and $\sum_P$ is determined. The gray values in $\sum_P$ are i nterpolated by bilinear interpolation, and these gray values, re-calculated by Eq. 5, are assigned to the corresponding pixel in Γ.

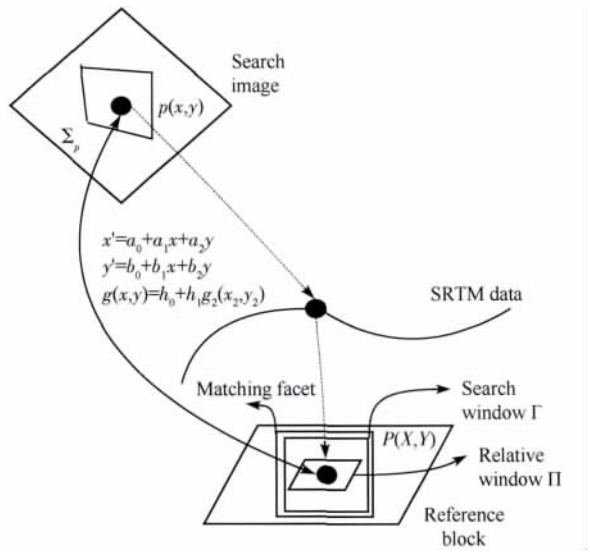

Fig. 4 The principle of the affine geometric transformation and linear radiometric transformation between the reference image and search image

3 EXPERIMENTS AND ANALYSIS

3.1 Test Data Description

To testify the performance of the proposed algorithm, two

sets of data acquired from Chinese satellites are taken as test data. Test one uses two long-strip images captured from ZY-3, which are scanned on the neighbor orbit, and cover Dalian city. Each long-strip covers 50×3800 km^2. The overlap between orbits is about 20%. The topography is mainly plains, including some residential areas and water areas. Test two uses two long-strip images captured from Mapping Satellite-1. covering Harbin city. Each long-strip covers 60×1200 km^2. The overlap between orbits is about 12%. The topography is mainly plains and mountain country, including some woodlands and farmlands. The test data information is shown in Table 3.

Table 3 The test data information for Mapping Satellite-1 and ZY-3

Parameter	Test one			Test two		
Sensor	ZY-3			Mapping Satellite-1		
Camera	Forward sight	Nadir sight	Backward sight	Forward sight	Nadir sight	Backward sight
Focal length/mm	1833	1700	1833	717	650	717
GSD/m	3.5	2.1	3.5	5.0	5.0	5.0
Camera angle/(°)	22.0	0.0	−22.0	25.0	0.0	−25.0
Pixel size/mm	0.0117	0.0070	0.0117	0.0065	0.0065	0.0065
Image wideth/pixel	16300	24530	16300	12000	12000	12000
Image height/pixel	1090556	1845245	1085436	142862	238100	142862
Data quantity/GB	34.75	88.46	34.58	4.46	7.31	4.46
Imaging time	Orbit one: 2012-01-11 Orbit two: 2012-01-16			Orbit one: 2010-10-17 Orbit two: 2010-10-30		

3.2 Performance comparison of main matching algorithms

To evaluate the performance of the proposed algorithm, two main algorithms are introduced for comparison: (1) LS-SIFT: the least square matching based on SIFT (Silveiva, et al., 2008); (2) AM-RFM: automatic matching of high resolution satellite images based on RFM (Ji & Yuan, 2010). After image matching, the precise orbit and attitude parameters, calculated by bundle block adjustment, are used to forward intersection for all matches. Through reverse projecting onto long-strip images, the image residual of every match is achieved, as shown in Table 4.

Table 4 Performance comparison of the two main algorithms and the proposed algorithm

Test	Algorithm	Number of feature points	Number of matches	Number of matches in adjacent orbits	Number of matches after mismatches elimination	RMS/pixel
Test one	Proposed algorithm	384718	300120	30794	281856	0.53
	LS-SIFT	214681	131240	9412	97286	1.43
	AM-RFM	384718	287415	18758	173394	1.28
Test two	Proposed algorithm	128480	111842	14836	104285	0.47
	LS-SIFT	112430	62473	5381	50178	1.18
	AM-RFM	128480	103820	8641	76841	1.14

Table 4 illustrates the statistics of the matching results, and we can conclude as below.

(1) For LS-SIFT, the rate of mismatches is between 20% and 26%. Through manually checking, almost all of them are mismatches. Moreover, after mismatches elimination, the RMS keeps between 1.18 and 1.43 pixels. It indirectly shows that the accuracy of this method is low.

(2) For AM-RFM, the number of matches in adjacent orbits increases obviously, but the rate of mismatches is also rises, even above 40%. This method used approximate epipolar constraint, but was dependent on accuracy of direct location, and the search area only considers vertical direction. The determination of the matching window only considered perpendicular to the core line direction, and the search interval for nuclear line direction is set too small. In addition, the slope of the epipolar determines image resample of local window. This method cannot eliminate local distortion.

(3) For the proposed algorithm, the rate of mismatches is less than 10%, and the number of matches in adjacent orbits increases obviously. The RMS keeps within 0.5 pixels, and the matches are well distributed, better than the two algorithms. Fig. 5 shows the matching results of the two test data.

4 CONCLUSION

In this paper, a practical matching algorithm is presented for processing long-strips of Chinese satellite images. Based on global SRTM data, this algorithm provides a complete solution for multiple images of different GSD, visual angels and time phases in parallel environment. First, a long-strip imag is divided into image blocks at a physical blocking mechanism. These overlapping and independent blocks provide possibility of parallel

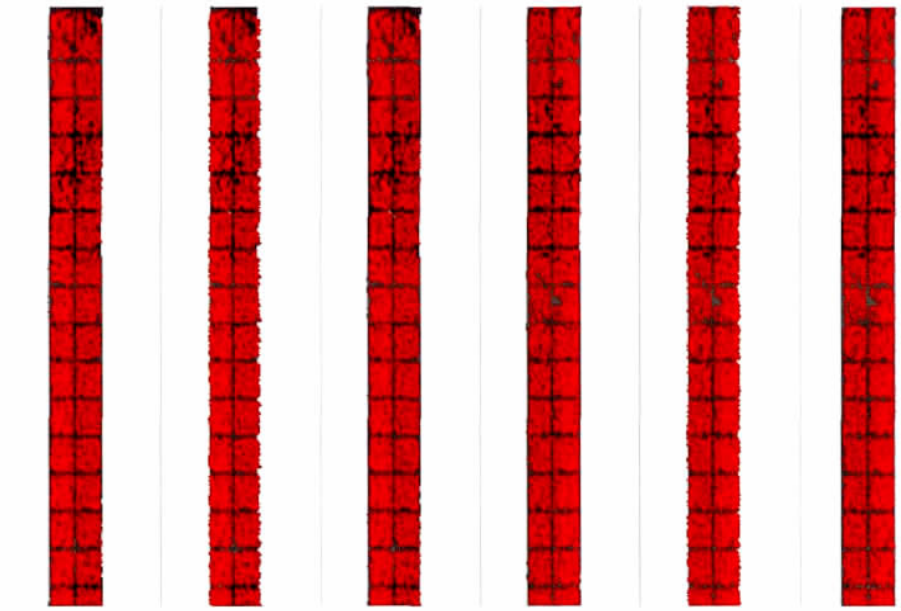

(a) General distribution map

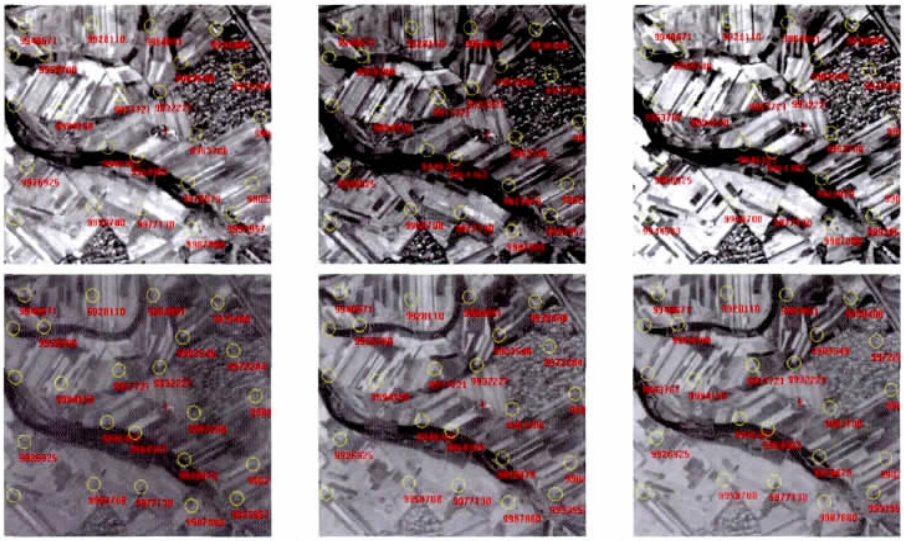

(b) Local enlarged drawing of more than six overlaps

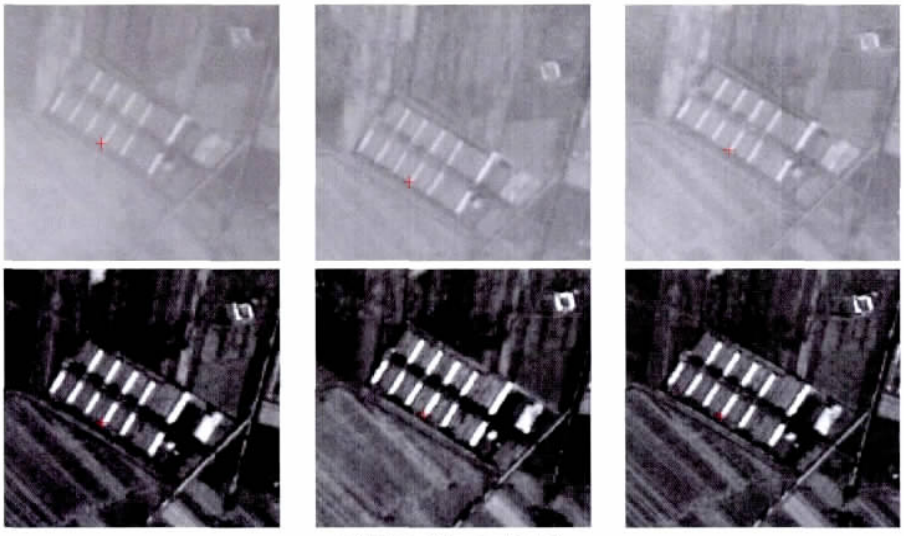

(c) Enlarged drawing for 1:3

Fig. 5 Matches distribution of test two

computation. Second, LBP/C measure is introduced to select the optimal features, which ensures the stability of matching. Third, through the global SRTM data, the true topographic relief covered by these blocks is obtained. Based on this true topographic relief, the approximate epipolar line is generated to c onstrain search scope. Fourth, along the epipolar line, local g eometric and radiative distortion is corrected. Finally, this paper integrates the matching flow and strategy. According to the characteristic of Chinese satellite data, a matching scheme is p roposed.

What deserves to be mentioned is that, the algorithm has been applied to the ground system of ZY-3, and the results are stable and reliable. We will continue this research in future to bring to fruition matching algorithms that will support various satellite sensors and perhaps various imaging modes.

REFERENCES

Cheng C Q, Deng K Z, Sun Y S and Li X T. 2010. Study of block adjustment for long-strip satellite CCD images. Acta Geodaetica et Cartographica Sinica, 39(2): 162 – 168

Cheng L, Gong J Y, Yang X X, Fan C and Han P. 2008. Robust affine invariant feature extraction for image matching. IEEE Geoscience and Remote Sensing Letters, 5(2): 264 – 250 [DOI: 10.1109/LGRS.2008.915599]

Gruen A and Baltsavias E P. 1988. Geometrically constrained multiphoto matching. Photogrammetry Engineering and Remote Sensing, 54(5): 633 – 641

Harris C and Stephens M A. 1998. Combined corner and edge detection. Proceeding of 4th Alevy Vision Conference, Mancherster: 147 – 151

Ji S P and Yuan X X. 2010. Automatic matching of high resolution satellite images based on RFM. Acta Geodaetica et Cartographica Sinica, 39(6): 592 – 598

Li F F, Jia Y H, Xiao B L and Zhang Q. 2010. A multi-sensor image registration algorithm based on line features and SIFT Points. Geomatics and Information Science of Wuhan University, 35(2): 233 – 236

Ojala T, Pietikainen M and Maenpaa T. 2002. Multi-resolution gray-scale and rotation invariant texture classification with local binary patterns. IEEE Transactions on Pattern Analysis and Machine Intelligence, 24(7): 971 – 987 [DOI: 10.1109/TPAMI.2002.1017623]

Silveira M, Feitosa R and Jacobsen K. 2008. A hybrid method for stereo image matching. The International Archives of the Photogrammetry, Remote Sensing and Spatial Information Science. Beijing: 37(B1): 895 – 901

Xie J F. 2009. The Critical Technology of Data Processing of Satellite Attitude Determinati-on Based on Star Sensor. State Key Laboratory for Information Engineering in Surveying Mapping and Remote Sensing, Wuhan University, 6

Xiong Z and Zhang Y. 2009. A novel interest-point-matching algorithm for high-resolution satellite images. IEEE Transaction on Geoscience and Remote Sensing, 47(12): 4189 – 4200 [DOI: 10.1109/TGRS.2009.2023794]

Zhang G, Chen T, Pan H B and Jiang W S. 2011. Patch-based least squares image matching based on rational polynomial coefficients model. Acta Geodaetica et Cartographica Sinica, 40(5): 592 – 597

Zhang L and Gruen A. 2006. Multi-image matching for DSM generation from IKONOS imagery. ISPRS Journal of Phototgrammetry and Remote Sensing, 60(3): 195 – 211 [DOI: 10.1016/j.isprsjprs.2006.01.001]

Zhang J Q and Hu A W. 2007. Method and precision analysis of multi-baseline photogrammetry. Geomatics and Information Science of Wuhan University, 32(10): 847 – 851

Zhang Y J and Zhang Y. 2005. Analysis of precision of relative orientation and forward intersection with high-overlap images. Geomatics and Information Science of Wuhan University, 30(2): 126 – 130

Zhang Y J, Zheng M T, Xiong J X, Lu Y and Xiong X. 2013. On-orbit geometric calibration of ZY-3 three-line array imagery with multistrip data sets. IEEE Transactions on Geoscience and Remote Sensing, 51(9): 1 – 11 [DOI: 10.1109/TGRS.2013.2237781]

Zhu Q, Wu B and Zhao J. 2005. A reliable image matching method based on self-adaptive triangle constraint. Chinese Journal of Computers, 10(28): 1735 – 1739

Zhu Z W, Shen Z F and Luo J C. 2011. Parallel remote sensing image registration based on improved SIFT point feature. Journal of Remote Sensing, 15(5): 1024 – 1039

SRTM 高程数据辅助的国产卫星长条带影像匹配

熊金鑫，张永军，郑茂腾，叶沅鑫

武汉大学 遥感信息工程学院，湖北 武汉 430079

摘 要: 针对国产卫星数据特点及长条带影像匹配困难问题，提出了一种基于全球 SRTM 数据的影像匹配方法。本文探讨了长条带影像物理分块机制，并引入 LBP/C 算子实现了兴趣点的筛选。在全球 SRTM 数据的辅助下，采用投影轨迹法，建立了近似核线方程。沿核线方向，进行局部畸变改正，进而消除匹配窗口的几何变形与辐射差异，利用金字塔匹配策略，逐层进行相关匹配。最后，在原始层引入 MPGC(Multi-photo Geometrically Constrained Matching) 算法与 RANSAC(Random Sample Consensus) 算法，进行精化匹配，并剔除误匹配点。文中综合运用了小面元几何纠正法与基于控制网的匹配生长算法，从而提高了匹配点的精度与均匀性。本文方法可在并行环境下全自动实现不同分辨率、不同视角、不同时相的多轨道长条带影像匹配，获得高精度的同名点观测值。以天绘一号与资源三号卫星影像作为试验数据，与现有匹配算法进行对比结果表明该算法具有较好的鲁棒性，能够达到较高的匹配精度。

关键词: 长条带，SRTM，影像匹配，天绘一号，资源三号

中图分类号: P23 **文献标志码**: A

引用格式: 熊金鑫，张永军，郑茂腾，叶沅鑫. 2013. SRTM 高程数据辅助的国产卫星长条带影像匹配. 遥感学报，17(5)：1103－1117

Xiong J X，Zhang Y J，Zheng M T and Ye Y X. 2013. An SRTM assisted image matching algorithm for long-strip satellite imagery. Journal of Remote Sensing，17(5)：1103－1117 [DOI: 10.11834/jrs.20132224]

1 引 言

随着航天技术的飞速发展，卫星定轨定姿及传感器关键技术的突破，在轨卫星数量急剧增加，越来越多的卫星数据应用到摄影测量领域(程春泉 等，2010) ，针对卫星影像的处理技术研究已成为现阶段的学术热点问题。由于卫星成像系统在空间飞行时，覆盖范围广，运行周期短，姿态稳定，多余观测多，卫星成像系统的上述特点对消除影像匹配中“病态解”(朱庆 等，2005) ，提高匹配精度与可靠性，具有重要意义。此外，卫星搭载的恒星定位仪与星敏器能够获得固定采样间隔下的扫描行姿轨数据(Zhang 等，2013) ，如通过几何约束方法，缩小匹配搜索范围，可获得相对可靠的未知参数初始值。由于卫星成像系统一般采用推扫式 CCD 线阵成像方式，具有不完全中心投影成像的几何特点，其成像的几何特征较传统的中心透视投影复杂。并且多视传感器(如前/正/后视) 的交会角、焦距、地面分辨率等存在差异，导致影像间存在复杂的几何与辐射畸变。卫星成像系统的上述特征为卫星影像的匹配研究带来了巨大挑战。

朱志文等人(2011) 针对遥感影像匹配算法存在内存消耗多、运算速度慢的问题，在 SIFT(Scale-Invariant Feature Transform) 算子的基础上，进行了改进，该算法可在并行环境下运行，提高了计算效率与匹配精度。但该算法对于大范围的遥感影像匹配适用性不强，可靠性和有效性有待进一步检验。李芳芳等人(2010) 提出了利用线特征与点特征相结合的遥感影像匹配方法，该方法利用线特征约束法获取高精度点特征，避免了几何差异与辐射差异造成的配准误差。该算法计算量较大，且线特征无法自动提取。季顺平和袁修孝等人(2010) 提出了基于 RFM(Rational Function Model) 的高分辨率卫星遥感影像匹配方法，通过 RFM 模型预测初始同名点，在

收稿日期: 2012-07-27; 修订日期: 2013-04-11; 优先数字出版日期: 2013-04-18

基金项目: 国家高技术研究发展计划(863 计划) (编号: 2012AA12A301，2013AA12A401) ; 国家自然科学基金(编号: 41071233) ; 中央高校基本科研业务费专项资金(编号: 201121302020004) ; 教育部博士研究生学术新人奖(编号: 5052011213018)

第一作者简介: 熊金鑫(1987—) ，男，博士研究生，研究方向主要为航空航天摄影测量、多源影像的联合匹配。E-mail: einbetter1995@hotmail.com

通信作者简介: 张永军(1975—) ，男，教授，主要从事数字摄影测量与遥感、计算机视觉方面的研究。E-mail: zhangyj@whu.edu.cn

近似核线约束下,进行金字塔影像匹配。该算法实现了高分辨率卫星影像的全自动匹配,但匹配正确率不够理想,且匹配精度有待提高。Zhang 和 Gruen (2006) 提出了几何约束互相关的匹配思想,在多基线情况下,基于高分辨率遥感影像生成了高精度 DEM(Digital Elevation Model) ,但该算法依赖于精确姿态轨道参数获得的大致准确的同名预测点。Silveira 等人(2008) 提出了结合特征匹配与灰度匹配的自动匹配算法,该算法利用 SIFT 算子,提供种子点,以种子点为基础,利用区域增长,进行最小二乘匹配。该算法适用于平坦地形下的影像匹配,但对居民地、山地、丘陵等复杂地形影像匹配效果较差。

综上所述,现有的影像匹配算法主要针对国外卫星同轨或异轨立体影像,而针对国产卫星影像特点的匹配算法研究还有待深入。国产卫星影像具有如下特点: 星敏器技术尚未成熟,直接定位精度有限(谢俊峰, 2009) ; 与国外卫星相比,国内卫星影像信息量较贫乏,纹理不够丰富,影像内部畸变差异较大; 国产卫星飞行过程中的直传数据一般为大范围的长条带线阵影像,如果利用分景后的影像进行影像匹配及区域网平差,则实际生产中,景与景之间平差精度很难保持一致,从而出现影像拼接问题。如果直接利用长条带影像进行匹配处理可对长条带影像整体纠正,则有利于消除影像拼接问题,并保证稀少控制点或无控地区的定位精度。因此,如何利用国产卫星长条带影像实现高精度自动匹配,为后续处理提供准确可靠的同名点观测值,是现阶段国产卫星影像亟待解决的前沿问题之一。

本文提出了一种基于全球 SRTM 数据的国产卫星长条带影像匹配算法。基本思想是: 在每一轨道内,将最接近于垂直摄影的影像作为基准影像,采用物理分块机制对基准影像进行分块处理,将基准影像分割为独立且具有一定重叠关系的基准影像块; 利用 Harris 算子在基准影像块上分别提取兴趣点,引入 LBP/C 算子(Ojala 等, 2002) 筛选兴趣点,保留局部纹理信息丰富的兴趣点作为待匹配点; 通过 SRTM 数据获得基准影像块对应的真实高程范围及搜索步距; 基于投影轨迹法建立近似核线,在近似核线上,改正局部畸变,消除窗口间的几何变形与辐射差异; 引入金字塔匹配策略,在顶层匹配完成后,前方交会获得匹配点的物方坐标,构建初始 DSM(Digital Surface Model) ,得到更为精确的高程信息,从而缩小高程搜索范围,并利用初始匹配点精化畸变模型参数,降低下一层匹配的计算量,提高核线预测精度与相关匹配的可靠性。当传递到原始层影像时,利用 Xiong (2009) 提出的基于控制网的匹配生长算法对匹配点进行加密,保证纹理贫乏区域的匹配点分布均匀,采用多片最小二乘匹配(MPGC) (Grue 和 Baltsavias, 1988) 实现匹配点位的精化,最后基于 RANSAC 算法,利用光束法前方交会(张剑清和胡安文, 2007; 张永军和张勇, 2005) 检测并剔除误匹配点,保证匹配结果正确性。

2 高精度自动匹配策略及方案

基于上述认识,针对国产卫星影像特点,设计了基于 SRTM 数据的长条带影像联合匹配方案(图 1) 。算法的具体流程如下:

(1) 基准影像预处理: 选取接近于垂直摄影的影像作为基准影像,采用物理分块机制得到相互独立的基准影像块。对每一影像块提取 Harris 兴趣点,利用 3.2 节中所提方法筛选兴趣点。基于全球 SRTM 数据通过像地正反投影,获得基准影像块在搜索长条带影像上对应的影像范围,建立金字塔影像。

(2) 匹配策略: 利用 3.3 所提方法生成兴趣点对应的近似核线,在金字塔顶层,以兴趣点为中心,利用 3.4 所提方法,经影像重采样实现对相关窗口与搜索窗口间的差异补偿。利用相关系数法匹配完成后,前方交会获得匹配点的物方坐标,构建初始 DSM,得到更为精确的高程信息,并精化差异补偿模型,将其传递到下一金字塔层进行匹配。经过迭代,最终实现原始层影像的粗匹配。

(3) 匹配点精化与剔除: 当原始影像层匹配完成后,利用匹配生长算法,对兴趣点进行加密,并采用 MPGC 算法,精化匹配点位。基于 RANSAC 算法,利用光束法前方交会,得到随机采样点的前方交会精度,将高于 3 倍前方交会中误差的点作为误匹配,予以剔除。

3 基于 SRTM 高程数据辅助的国产卫星长条带影像匹配

3.1 基准影像物理分块机制

由于长条带影像数据量过大,无法将其加载到内存中进行整体处理。需要通过分块方式将影像分割为独立且具有一定重叠关系的基准影像块,以影像块为单位,进行后续处理。通过影像分块处理,块

与块之间相互独立,在多机多核的情况下实现分布式并行匹配。

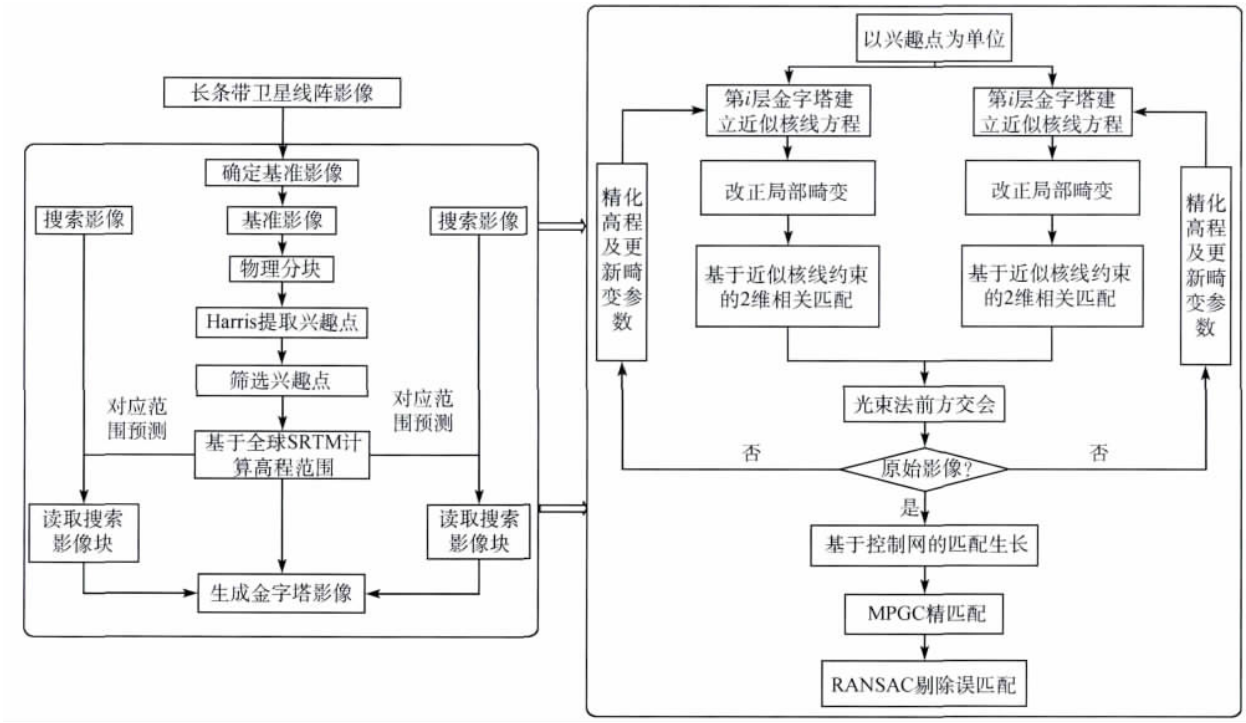

图1 基于 SRTM 数据的国产卫星长条带影像联合匹配方案

将最接近于垂直摄影的影像作为基准影像,将基准影像块大小设为 12000×12000 像元,为避免临近影像边缘的影像块出现越界现象,引入自动控制影像分块尺寸策略。建立影像分块的索引机制,记录每个基准影像块与原始影像的对应关系。

考虑到分块影像边界连续问题,物理分块时,块与块之间在列与行方向上均具有一定重叠,保证分块影像边界存在一定数量的匹配点,如图 2 所示。

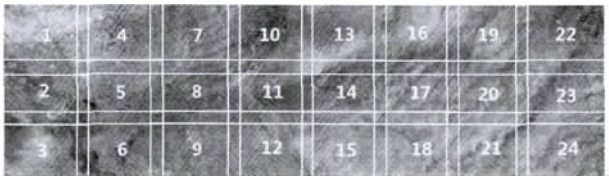

图2 基准长条带影像物理分块示意图

3.2 筛选兴趣点

Cheng 等人(2008)指出影像纹理信息量与影像可匹配性之间存在很强的相关性,尽管地表景观不同,但均表现出匹配正确率随纹理信息量增大而增大的趋势。LBP/C 算子可以统计分析影像局部纹理的空间特征与反差,很好地描述纹理信息(Ojala 等,2002)。利用 LBP/C 算子筛选兴趣点,可有效提高同名点的匹配正确率。

在基准影像块上,采用 Harris 算子(Harris 和 Stephens,1998)提取兴趣点,利用 LBP/C 算子统计兴趣点的 LBP 图与 LC 图的像元值分布,得到 LBP/C 2 维直方图,直方图描述了兴趣点局部纹理空间分布特征和局部纹理反差。本文在一组天绘一号同轨立体像对上人工选取 133 个检查点、在一组资源三号异轨立体像对上选取 154 个检查点,将检查点作为待匹配点,用于判断匹配的正确性。如图 3 所示,当检查点位于纹理贫乏区域,其邻域内像元点近似,LC 值在 0 附近。表 1 描述了分别位于纹理贫乏区域与纹理丰富区域检查点的匹配结果,位于纹理丰富区域的匹配成功率与正确率明显高于纹理贫乏区域。因此,利用上述方法可有效剔除纹理贫乏区域的点位,提高整体的匹配正确率。

表1 不同纹理区域下兴趣点匹配结果对比

立体像对	纹理区域	检查点数	匹配成功率/%	匹配正确率/%
天绘一号	贫乏区域	47	70.2	51.5
	丰富区域	86	79.0	75.3
资源三号	贫乏区域	61	75.4	61.2
	丰富区域	93	93.5	82.9

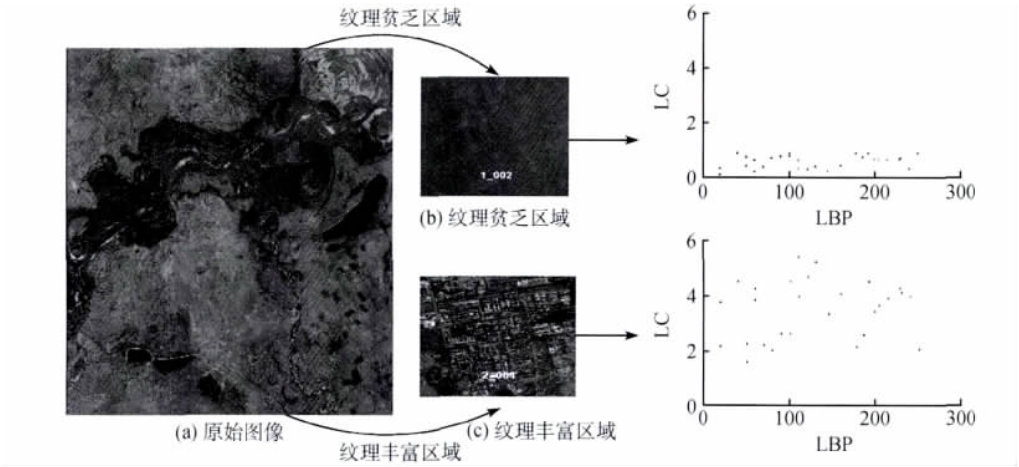

图 3 影像中纹理贫乏区域与纹理丰富区域的 LBP/C 直方图对比图

3.3 基于 SRTM 数据生成近似核线

在推扫式卫星影像中,各扫描行均有自身的投影中心和姿轨参数,因此并不存在严格意义上的核线定义(季顺平和袁修孝, 2010)。张过等人(2011)分析了高程误差对于影像匹配结果的影响,指出高程初值和实际值相差越小,匹配结果越好。为消除高程误差对于核线预测精度的影响,利用全球 SRTM 数据获得影像覆盖区域的真实地形起伏,利用地面高程变化生成近似核线,作为匹配的约束条件。

以每一基准影像块为单位,根据卫星参数信息,计算出影像块所覆盖的概略地理范围,本文使用 SRTM 90 m 分辨率的全球高程数据,获取该范围的最大高程 $H_{\max}$、最小高程 $H_{\min}$。

为保证近似核线的拟合精度,需要选取合适的地面高程变化幅度,即高程搜索步距。将基准影像块中待匹配点分别以 $H_{\max}$、$H_{\min}$ 作为高程投影到待匹配影像上,得到投影点影像坐标 $(x_{\max}, y_{\max})$、$(x_{\min}, y_{\min})$。高程搜索步距按照以下公式求得:

$$Length = \sqrt{(x_{\max} - x_{\min})^2 + (y_{\max} - y_{\min})^2} \quad (1)$$

$$H_{\text{pitch}} = (H_{\max} - H_{\min}) / Length \quad (2)$$

式中,$Length$ 为点位在影像上的距离,H_{pitch} 为高程搜索步距。

利用式(3)获得地面高程值,采用投影轨迹法在待匹配影像上生成近似核线,在实际影像范围内,该核线为曲线。

$$H_i = H_{\min} + i \cdot H_{\text{pitch}} \quad (i = 1, 2, \cdots, n, H_i \leqslant H_{\max}) \quad (3)$$

3.4 基于近似核线约束的相关匹配

在待匹配影像上获得兴趣点对应的近似核线后,理论上讲,同名点应位于近似核线上,利用相关系数法,沿核线方向进行 1 维匹配即可。但由于近似核线存在预测误差,实际上同名点位与近似核线之间存在一定的偏差。近似核线预测精度主要受相机内部畸变、姿态轨道直接定位精度、SRTM 高程误差等因素影响。利用资源三号前视与后视影像构成像对 1、天绘一号前视与后视影像构成像对 2,手工选取同名点作为检查点,综合考虑上述因素的影响,将真实点位到核线的最近距离作为偏差 Δ,将 X 方向与 Y 方向的近似核线预测误差列于表 2。

表 2 核线预测误差表

立体像对	检查点个数	X 方向最大偏差/(像元)	X 方向平均偏差/(像元)	Y 方向最大偏差/(像元)	Y 方向平均偏差/(像元)
像对 1	15	10.2	4.8	85.5	76.3
像对 2	21	54.6	32.2	44.9	25.1

从表 2 看出,X 方向的最大预测误差可达到 54 个像元左右,而 Y 方向的预测误差最大可达到 85 个像元左右。在这里,采用金字塔分层匹配策略,逐层缩小搜索范围,使匹配结果逐层精化,避免因预测误差过大、搜索范围过小导致的匹配失效现象。本文利用平均滤波法以 3×3 像元窗口为模板,建立 3 层金字塔,顶层金字塔的相关窗口为 5×5 像元,搜索窗口在 x 方向为 11 像元,y 方向为 35 像元。利用归一化相关系数进行 2 维核线匹配,阈值设为 0.65,在核线上对所有超过阈值的相关系数进行二次曲线拟合,极大值对应的匹配点即为初始同名点。通过逐层传递,每一层中搜索窗口缩小 2×6 像元,阈值提高 0.05。在原始层影像上,搜索窗口为 5×13,阈值为 0.8。

由于卫星在高空摄影时,受 CCD 相机弯曲、位移等因素影响,影像内部畸变差异较大,无法用同一数学模型描述内部畸变特征。并且受分辨率、焦距、交会角、地形变化等影响,导致影像间几何变形较大。因此,在基准影像块定义相关窗口后,如果直接利用上述方法进行相关匹配,在搜索影像上匹配窗口会出现不规则,甚至不连续的情况,易造成匹配失效或误匹配的现象,因此无法直接进行相关匹配。

如图 4 所示,以兴趣点 P 为中心,定义一个矩形小面元,该面元大小要不小于相关窗口与匹配窗口大小。通过 SRTM 内插出的高程及姿轨参数,将小面元 4 个角点投影到物方面元,再依据像地坐标反算,将其分别投影到搜索影像上,得到 $\sum_p$。

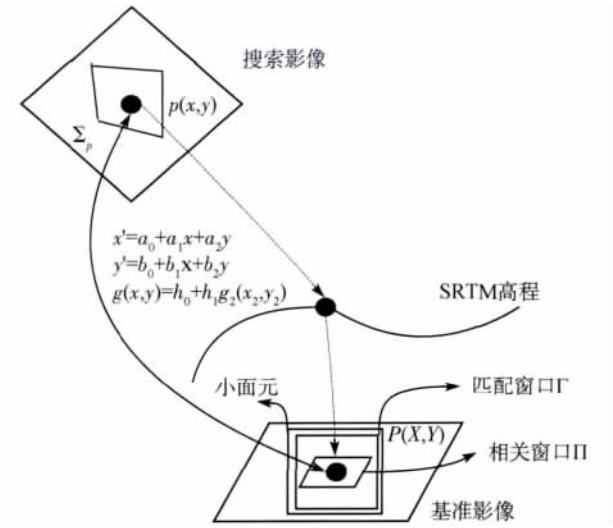

图 4 匹配窗口局部畸变差异消除原理图

依据上述 4 个角点的对应关系,利用仿射变换模型来描述影像几何变形,线性灰度畸变参数来改正辐射畸变。在基准影像小面元内,以兴趣点为中心定义相关窗口与匹配窗口,将匹配窗口中每个像元点利用畸变改正模型解算到搜索影像上,经过重采样后将灰度值赋给匹配窗口,从而消除窗口变形对匹配结果的影响,保证相关匹配的稳定性。

4 试验及其结果分析

4.1 试验设计

为验证算法的可行性与适用性,选取两组国产长条带卫星影像进行匹配试验。试验 1 采用拍摄于大连地区的两轨资源三号卫星邻轨长条带影像作为试验数据,每轨影像的覆盖范围为 50×3800 km^2,轨道间重叠度为 20%,地形主要以平原为主,居民地、水域居多,包含山地、丘陵地带。试验 2 则采用拍摄于哈尔滨地区的两轨天绘一号卫星邻轨长条带影像作为试验数据,每轨影像的覆盖范围为 60×1200 km^2,轨道间重叠度为 12%,地势变化较为缓慢,主要以平原、海拔较低的丘陵为主,森林、农田居多。具体试验数据参数见表 3 所示。

表 3 试验数据参数描述

参数信息	试验 1			试验 2		
传感器	资源三号			天绘一号		
相机	前视	正视	后视	前视	正视	后视
焦距/mm	1833	1700	1833	717	650	717
GSD/m	3.5	2.1	3.5	5.0	5.0	5.0
摄影视角/°	22.0	0.0	-22.0	25.0	0.0	-25.0
像元/mm	0.0117	0.0070	0.0117	0.0065	0.0065	0.0065
影像宽/像元	16300	24530	16300	12000	12000	12000
影像高/像元	1090556	1845245	1085436	142862	238100	142862
数据量/GB	34.75	88.46	34.58	4.46	7.31	4.46
摄影时间		轨道 1:2012-01-11 轨道 2:2012-01-16			轨道 1:2010-10-17 轨道 2:2010-10-30	

4.2 影像匹配算法对比

为评价本文所提方法的性能,这里同时采用两种现有主流的遥感卫星影像匹配算法进行对比试验:(1) Silveira 等人(2008)提出的基于 SIFT 的最小二乘匹配;(2) 季顺平和袁修孝等人(2010)提出

的基于 RFM 的高分辨率卫星影像匹配。上述匹配方法均引入金字塔匹配策略,皆采用 C + + 语言编写。为定量分析算法的匹配精度,利用区域网平差解算后的精密轨道姿态参数将所有匹配点进行前方交会,获得其物方坐标,之后反投影到对应影像上,计算出各匹配点的像方残差,最终得到匹配的像方中误差。以上两种方法与本文方法匹配结果一并列于表 4。

表 4 不同方法下影像匹配结果对比

试验	匹配方法	兴趣点数目	匹配点数目	异轨匹配点数目	剔除后匹配点数目	像方中误差/像元
试验 1	本文方法	384718	300120	30794	281856	0.53
	方法 1	214681	131240	9412	97286	1.43
	方法 2	384718	287415	18758	173394	1.28
试验 2	本文方法	128480	111842	14836	104285	0.47
	方法 1	112430	62473	5381	50178	1.18
	方法 2	128480	103820	8641	76841	1.14

4.3 结果分析

分析表 4 试验结果可以得出:

采用方法 1,RANSAC 检测出的误匹配率在 20%—26%,表明这些匹配点经前方交会无法集中于一点,交会误差较大,这也间接说明了该方法的匹配精度有限。通过对剔除的点位进行随机的人工检查,这些匹配点几乎都属于误匹配点。另外,在剔除误匹配后该方法的像方中误差在 1.18—1.43 个像元,究其原因,主要由于长条带影像间几何变形大且不均匀,通过在顶层进行 SIFT 初始匹配而计算得到的基本矩阵,其约束性有限,无法正确描述局部的几何畸变。

而采用方法 2,异轨影像间匹配点数明显增多,但误匹配检测率也明显上升,试验 1 达到了 40%。该方法虽然引入了近似核线约束,但对于核线精度过于依赖,匹配窗口的确定只考虑了垂直于核线方向,而对于核线方向的搜索区间设置过小。另外,该方法根据核线斜率决定局部匹配窗口的重采样,因此,无法完全消除局部几何畸变,从而降低了匹配可靠性,其像方中误差在 1.14—1.28 个像元之间,匹配结果无法令人满意。

采用本文方法,明显降低了误匹配检测率,误匹配检测率可保持在 10% 以内,且异轨影像间的匹配点数明显增多,匹配的像方中误差也保持在 0.5 像元以内,匹配点位分布均匀,匹配结果优于以上两种方法。由于篇幅限制,图 5 只显示了本文方法对于试验 2 数据的匹配结果图。

5 结 论

针对国产卫星数据特点及长条带影像匹配困难问题,本文在现有匹配算法的基础上,提出了一种基于全球 SRTM 数据的影像匹配方法,为多轨道长条带影像联合匹配提供了较为完善的解决思路。本文方法的特点在于:(1)利用物理分块的方式将长条带影像划分为相互独立的匹配任务,可在多机多核的环境下实现分布式并行匹配;(2)利用 LBP/C 算子对兴趣点进行筛选剔除,保证兴趣点匹配的高精度与可靠性;(3)在全球 SRTM 数据的辅助下,采用已有核线生成方法建立近似核线几何约束,极大地减少了由于高程误差造成的核线预测误差,并且定量分析了相关因素对于核线精度的影响,以此为条件,对匹配参数进行了设置;(4)通过匹配窗口的局部畸变改正,避免了相关窗口与搜索窗口间的几何与辐射差异,提高了匹配精度;(5)将匹配流程及匹配策略进行了整合与改进,为国产卫星多轨长条带影像全自动匹配提供了较为完善的匹配方案。

该方法已成功应用于资源系列卫星地面系统的建设中,在实际应用中匹配结果稳定可靠。通过利用天绘一号与资源三号卫星多轨长条带影像作为试验数据,并与目前普遍采用的两种遥感卫星匹配方法进行对比表明:本文方法能够在自动情况下实现不同分辨率、不同视角、不同时相的多轨道长条带影像的联合匹配,获得高精度的同名点观测值,为未来最大限度地联合对地观测数据进行大范围空中三角测量奠定基础。

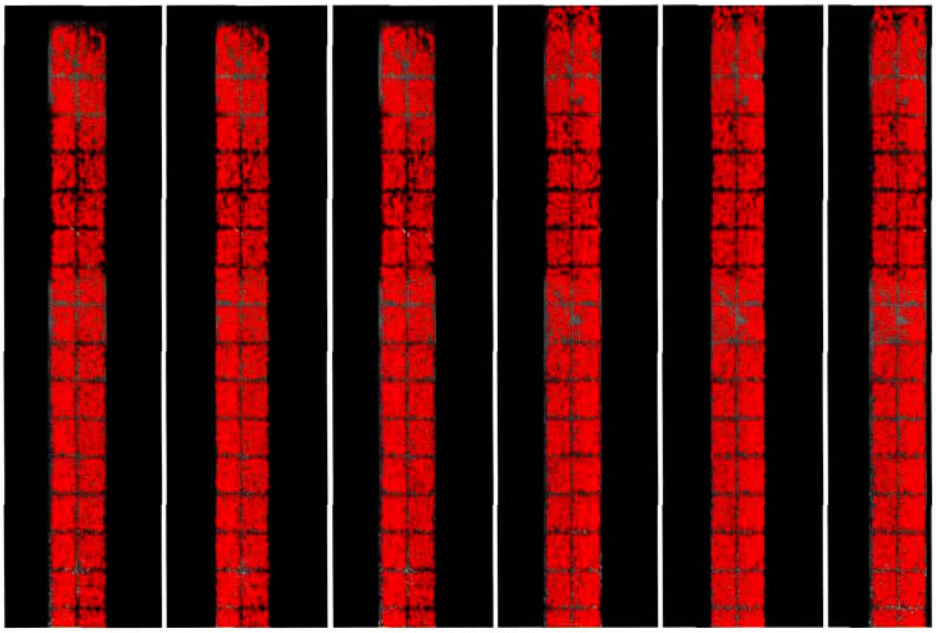

(a) 匹配点位总体分布图

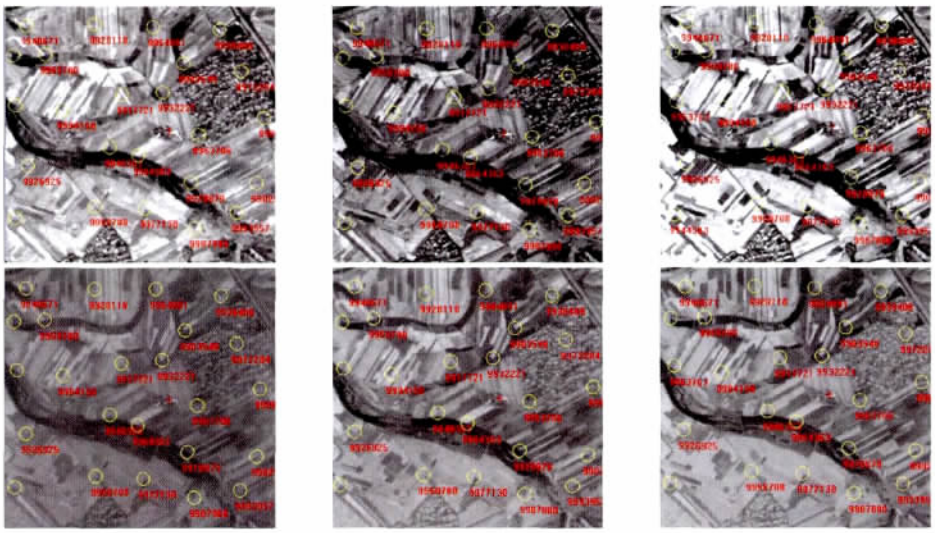

(b) 轨道间6度重叠匹配点局部放大图

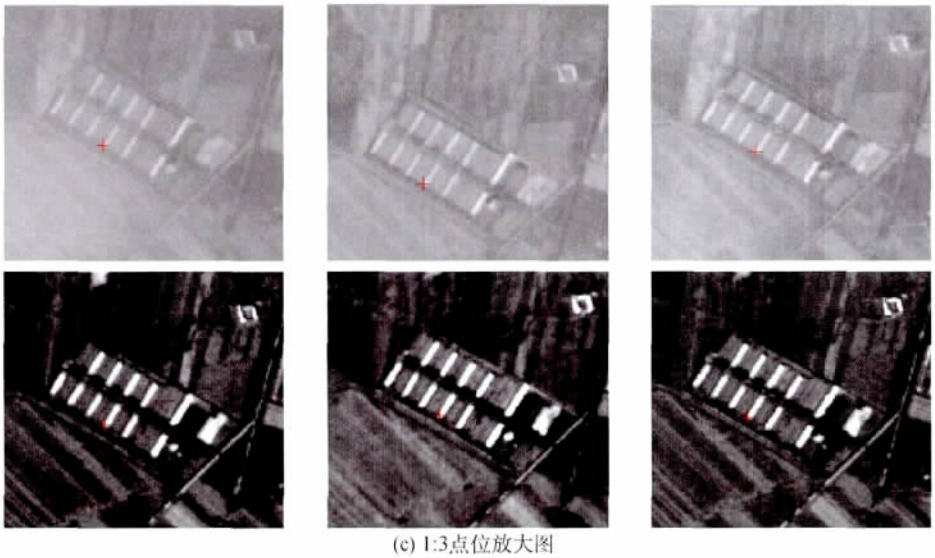

(c) 1:3点位放大图

图5 试验2点位分布图

参考文献(References)

程春泉，邓喀中，孙钰珊，李小涛. 2010. 长条带卫星线阵影像区域网平差研究. 测绘学报，39(2)：162－168

Cheng L，Gong J Y，Yang X X，Fan C and Han P. 2008. Robust affine invariant feature extraction for image matching. IEEE Geoscience and Remote Sensing Letters，5(2)：264－250 [DOI：10.1109/LGRS.2008.915599]

Gruen A and Baltsavias E P. 1988. Geometrically constrained multiphoto matching. Photogrammetry Engineering and Remote Sensing，54(5)：633－641

Harris C and Stephens M A. 1998. Combined corner and edge detection. Proceeding of 4th Alevy Vision Conference，Mancherster：147－151

季顺平，袁修孝. 2010. 基于 RFM 的高分辨率卫星遥感影像自动匹配研究. 测绘学报，39(6)：592－598

李芳芳，贾永红，肖本林，张谦. 2010. 利用线特征和 SIFT 点特征进行多源遥感影像配准. 武汉大学学报(信息科学版)，35(2)：233－236

Ojala T，Pietikainen M and Maenpaa T. 2002. Multi-resolution gray-scale and rotation invariant texture classification with local binary patterns. IEEE Transactions on Pattern Analysis and Machine Intelligence，24(7)：971－987 [DOI：10.1109/TPAMI.2002.1017623]

Silveira M，Feitosa R and Jacobsen K. 2008. A hybrid method for stereo image matching. The International Archives of the Photogrammetry，Remote Sensing and Spatial Information Science. Beijing：37(B1)：895－901

谢俊峰. 2009. 卫星星敏感器定姿数据处理关键技术研究. 武汉大学：测绘遥感信息工程国家重点实验室，6

Xiong Z and Zhang Y. 2009. A novel interest-point-matching algorithm for high-resolution satellite images. IEEE Transaction on Geoscience and Remote Sensing，47(12)：4189－4200 [DOI：10.1109/TGRS.2009.2023794]

张过，陈钽，潘红播，江万寿. 2011. 基于有理多项式系数模型的物方面元最小二乘匹配. 测绘学报，40(5)：592－597

Zhang L and Gruen A. 2006. Multi-image matching for DSM generation from IKONOS imagery. ISPRS Journal of Phototgrammetry and Remote Sensing，60(3)：195－211 [DOI：10.1016/j.isprsjprs.2006.01.001]

张剑清，胡安文. 2007. 多基线摄影测量前方交会方法及精度分析. 武汉大学学报(信息科学版)，32(10)：847－851

张永军，张勇. 2005. 大重叠度影像的相对定向与前方交会精度分析. 武汉大学学报(信息科学版)，30(2)：126－130

Zhang Y J，Zheng M T，Xiong J X，Lu Y and Xiong X. 2013. On-orbit geometric calibration of ZY-3 three-line array imagery with multistrip data sets. IEEE Transactions on Geoscience and Remote Sensing，51(9)：1－11 [DOI：10.1109/TGRS.2013.2237781]

朱庆，吴波，赵杰. 2005. 基于自适应三角形约束的可靠影像匹配方法. 计算机学报，10(28)：1735－1739

朱志文，沈占峰，骆剑承. 2011. 改进 SIFT 点特征的并行遥感影像配准. 遥感学报，15(5)：1032－1039